Mononuclear Iron(II), Manganese(II), and Nickel(II) and Tetranuclear Iron(III) Complexes of a New Hexadentate Ligand

Navamoney Arulsamy,[1a] Jørgen Glerup,[1b] and Derek J. Hodgson*,[1a]

Department of Chemistry, University of Wyoming, Laramie, Wyoming 82071, and Chemistry Laboratory I, H. C. Ørsted Institute, Universitetsparken 5, DK-2100 Copenhagen Ø, Denmark

Received October 6, 1993®

The syntheses of the novel hexadentate nitrogen ligand 1,10-bis(2-pyridylmethyl)-1,4,7,10-tetraazadecane (bpteta), $C_{18}H_{28}N_6$, and of its complexes with iron(II), manganese(II), and nickel(II) are reported. The structures of the mononuclear complexes $[M(bpteta)](ClO_4)_2$ (M = Fe, Mn, Ni) and that of the tetranuclear iron(III) complex $\{[Fe_2(\mu\text{-}O)(\mu\text{-}OAc)_2]_2(\mu\text{-}bpteta)_2\}(ClO_4)_4$ have been determined by three-dimensional X-ray diffraction methods. The iron(II) complex $[Fe(bpteta)](ClO_4)_2$ (**1**) crystallizes in the space group $P2_1/c$ of the monoclinic system with four molecules in a cell of dimensions a = 12.496(2) Å, b = 12.148(2) Å, c = 16.800(3) Å, and β = 109.12(3)°. The nickel(II) complex $[Ni(bpteta)](ClO_4)_2$ (**3**) is isomorphous with the iron analogue, with cell dimensions a = 12.507(3) Å, b = 12.307(2) Å, c = 16.777(3) Å, and β = 108.80(3)°. The geometry at iron or nickel is six-coordinate pseudooctahedral, with pyridine nitrogen atoms mutually *cis* and *trans* to amine nitrogen atoms. The manganese(II) complex $[Mn(bpteta)](ClO_4)_2$ (**2**) also crystallizes in the space group $P2_1/c$ of the monoclinic system with four molecules in a cell of dimensions a = 13.869(3) Å, b = 8.710(2) Å, c = 20.710(4) Å, and β = 91.07(2)°. The geometry at manganese is trigonal prismatic. The tetranuclear iron(III) complex $\{[Fe_2(\mu\text{-}O)(\mu\text{-}OAc)_2]_2(\mu\text{-}bpteta)_2\}(ClO_4)_4$ (**4**) crystallizes in the space group $C2/c$ of the monoclinic system with four tetranuclear units in a cell of dimensions a = 23.414(5) Å, b = 22.669(5) Å, c = 14.017(3) Å, and β = 105.77(2)°. The complex is best described as a dimer of dimers, in which two $[N_3Fe(\mu\text{-}O)(\mu\text{-}OAc)_2FeN_3]$ cores are spanned by the bpteta ligands. The geometry at each iron center is roughly octahedral, with facial coordination of three nitrogen atoms from the bpteta ligands and three bridging oxygen atoms from the one μ-oxo and two μ-acetato groups. The Fe···Fe separation between the cores is 7.358 Å. The tetranuclear complex exhibits strong antiferromagnetic coupling with an exchange constant $J = -120$ cm^{-1}, a value similar to those for related complexes and close to that for methemerythrin. The three monomeric complexes **1**–**3** exhibit quasi-reversible redox couples at +0.750, +1.100, and +1.435 V (vs Ag/AgCl in acetonitrile), respectively, corresponding to the Fe(II) ↔ Fe(III), Mn(II) ↔ Mn(III), and Ni(II) ↔ Ni(III) processes. The tetranuclear complex **4** exhibits a single irreversible cathodic wave at –0.62 V, which is similar to the behavior of other known $[Fe_2(\mu\text{-}O)(\mu\text{-}OAc)_2]^{2+}$ complexes.

Introduction

Iron and manganese ions present at the active sites of various enzymes in the living systems play a central role in the diverse redox functions of the enzymes. Oxo-bridged diiron cores present in the invertebrate dioxygen carrier hemerythrin, ribonucleotide reductase, methane monoxygenase, and purple acid phosphatase are well characterized.[2] The presence of a (μ-oxo)bis(μ-carboxylato)diiron(III) core in methemerythrin and a (μ-oxo)(μ-carboxylato)diiron(III) core in *Escherichia coli* ribonucleotide reductase has been unambiguously demonstrated by X-ray analysis.[3,4] Manganese-containing enzymes have also attracted considerable attention. Manganese superoxide dismutase (Mn-SOD) which serves as a catalyst for superoxide dismutation in biological systems has been shown to contain a mononuclear manganese active site on the basis of X-ray analyses of several Mn-SOD enzymes.[5] Pseudocatalase is presumed to contain a dinuclear manganese active site on the basis of low-temperature ESR measurements of the enzyme[6] and electronic spectral features of synthetic model complexes containing the (μ-oxo)bis(μ-carboxylato)dimanganese(III/IV) core which mimic the electronic spectral features of the enzyme.[7] Similarly, the water-splitting enzyme photosystem II (PS II) is thought to contain a dinuclear or a tetranuclear manganese core at the active site from the EXAFS data of the enzyme. However, the photosystem is poorly understood and continues to attract current attention.

In order to elucidate the role of the metal ions in the redox functions of the natural systems mentioned above, a large number of model complexes have been synthesized and investigated.[5,9–13] We have previously used the tetradentate N_4 ligands bis(*N*,*N*'-(2-pyridylmethyl)ethane-1,2-diamine (bispicen) and tris(2-pyridylmethyl)amine (tmpa) and related ligands for the synthesis of various bis(μ-oxo)dimanganese(III/III), -(III/IV), and -(IV/IV), (μ-oxo)(μ-acetato)dimanganese(III/III), and (μ-oxo)(μ-acetato)diiron(III/III) complexes and studied their relevance as

* Abstract published in *Advance ACS Abstracts,* June 1, 1994.

(1) (a) University of Wyoming. (b) H. C. Ørsted Institute.
(2) (a) Sheriff, S.; Hendrickson, W. A.; Smith, J. L. *J. Mol. Biol.* **1987**, *197*, 273–296. (b) Vincent, J. B.; Olivier-Lilley, G. L.; Averill, B. A. *Chem. Rev.* **1990**, *90*, 1447–1467 and references therein.
(3) (a) Stenkamp, R. E.; Sieker, L. C.; Jensen, L. H.; Sanders-Loehr, J. *Nature (London)* **1981**, *291*, 263–264. (b) Stenkamp, R. E.; Sieker, L. C.; Jensen, L. H. *J. Am. Chem. Soc.* **1984**, *106*, 618–622.
(4) Nordlund, P.; Sjöberg, B. M.; Eklund, H. *Nature* **1990**, *345*, 593–598.
(5) Stallings, W. C.; Pattridge, K. A.; Strong, R. K.; Ludwig, M. L. *J. Biol. Chem.* **1984**, *259*, 10695–10699.
(6) Khangulov, S. V.; Barynin, V. V.; Melik-Adamyan, V. R.; Grebenko, A. I.; Voevodskaya, N. V.; Blyumenfel'd, L. A.; Dobryakov, S. N.; Il'yasova, V. B. *Bioorg. Khim.* **1986**, *12*, 741.
(7) (a) Sheats, J. E.; Czernuszewicz, R. S.; Dismukes, G. C.; Rheingold, A. L.; Petrouleas, V.; Stubbe, J.; Armstrong, W. H.; Beer, R. H.; Lippard, S. J. *J. Am. Chem. Soc.* **1987**, *109*, 1435–1444. (b) Wieghardt, K.; Bossek, U.; Ventur, D.; Weiss, J. *J. Chem. Soc., Chem. Commun.* **1985**, 347–349. (c) Wieghardt, K.; Bossek, U.; Bonvoisin, J.; Beauvillain, P.; Girerd, J.-J.; Nuber, B.; Weiss, J.; Heinze, J. *Angew. Chem., Int. Ed. Engl.* **1986**, *25*, 1030–1031.
(8) Penner-Hahn, J. E.; Fronko, R. M.; Pecoraro, V. L.; Yocum, C. F.; Betts, S. D.; Bowlby, N. R. *J. Am. Chem. Soc.* **1990**, *112*, 2549–2557.
(9) Armstrong, W. H.; Lippard, S. J. *J. Am. Chem. Soc.* **1983**, *105*, 4837–4838.
(10) Wieghardt, K.; Pohl, K.; Gebert, W. *Angew. Chem., Int. Ed. Engl.* **1983**, *22*, 727.
(11) (a) Kurtz, D. M., Jr. *Chem. Rev.* **1990**, *90*, 585–606. (b) Vincent, J. B.; Christou, G. *Adv. Inorg. Chem.* **1990**, *33*, 197–257.

0020-1669/94/1333-3043$04.50/0

models for the enzymes.[12,13] The studies have revealed that the tetradentate ligands lead to the formation of dinuclear manganese and iron complexes. It may be possible to synthesize tetranuclear iron and/or manganese complexes using hexadentate or octadentate ligands. Hence, as an extension of our investigation in this area, we have synthesized a new hexadentate N_6 ligand, namely, 1,10-bis(2-pyridylmethyl)-1,4,7,10-tetraazadecane, bpteta,

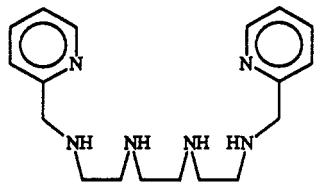

bpteta

as its hydrochloride salt and studied its coordination properties with various transition metal ions and its ability to form a tetranuclear iron(III) complex consisting of two independent (μ-oxo)(μ-acetato)diiron(III/III) cores. In this paper, we wish to report the synthesis and properties of the iron(II), manganese(II), and nickel(II) mononuclear complexes of the ligand and the tetranuclear iron(III) complex.

Experimental Section

Synthetic Methods. ***Caution!*** *The complexes described were isolated as perchlorate salts and should be handled as potentially explosive compounds.*

1,10-Bis(2-pyridylmethyl)-1,4,7,10-tetraazadecane Tetrahydrochloride Hydrate (bpteta·4HCl·H_2O). To a solution of pyridine-2-carboxaldehyde (4.28 g, 40 mmol) in ethanol (95%, 50 mL) was added triethylenetetramine hydrate (2.92 g, 20 mmol), and the solution was stirred overnight. Sodium borohydride (1.59 g, 42 mmol) was added in small portions to the solution, and the mixture was stirred for another 12 h. The reaction mixtrue was neutralized with concentrated HCl (pH 7–6.5) in an ice bath and filtered to remove the white solid formed. The yellow filtrate was further acidified to pH 2 and allowed to stand at 4 °C for 6 h. The white crystals formed were filtered off, washed with ethanol (95%), and air-dried. Yield: 7.2 g (73%). Anal. Calcd for $C_{18}H_{34}N_6Cl_4O$: C, 43.91; H, 6.96; N, 17.07; Cl, 28.80. Found: C, 43.87; H, 6.96; N, 17.03; Cl, 28.86. ^{1}H NMR (D_2O/DSS): δ 8.68 (d, 2H, pyridine H), 8.14 (t, 2H, pyridine H), 7.63–7.772 (m, 4H, pyridine H), 4.50 (s, 4H, pyridylmethyl), 3.54–3.60 (m, 12H, CH_2CH_2).

[Fe(bpteta)](ClO_4)$_2$ (1). Sodium acetate trihydrate (0.524 g, 4 mmol) was added to a solution of bpteta·4HCl·H_2O (0.492 g, 1 mmol) in absolute ethanol (20 mL). The mixture was stirred for 10 min and filtered. The filtrate was degassed and added to a solution of $Fe(ClO_4)_2$·$6H_2O$ (0.363 g, 1 mmol) in absolute ethanol (10 mL) under a nitrogen atmosphere. The dark-red solution was stirred briefly, and red crystals formed after it stood overnight under a nitrogen atmosphere. The crystals were filtered off in air, washed with a small quantity of cold absolute ethanol, and air-dried. Yield: 0.268 g (46%). Anal. Calcd for $C_{18}H_{28}Cl_2FeN_6O_8$: C, 37.07; H, 4.84; N, 14.41; Cl, 12.16. Found: C, 36.81; H, 4.89; N, 14.31; Cl, 11.97.

[Mn(bpteta)](ClO_4)$_2$ (2). Sodium acetate trihydrate (0.524 g, 4 mmol) was added to a solution of bpteta·4HCl·H_2O (0.492 g, 1 mmol) in absolute ethanol (20 mL). The mixture was stirred for 10 min and filtered. Mn(ClO_4)$_2$·$6H_2O$ (0.362 g, 1 mmol) was added to the filtrate, and the colorless solution was stirred in air briefly; colorless crystals formed in less than 24 h. The crystals were filtered off, washed, and dried as above. Yield: 0.360 g (62%). Anal. Calcd for $C_{18}H_{28}Cl_2MnN_6O_8$: C, 37.13; H, 4.85; N, 14.43; Cl, 12.18. Found: C, 37.25; H, 4.85; N, 14.48; Cl, 12.14.

[Ni(bpteta)](ClO_4)$_2$ (3). The nickel(II) complex was synthesized as described for the manganese(II) complex using Ni(ClO_4)$_2$·$6H_2O$ (0.366 g, 1 mmol). The complex crystallized from the reaction mixture as violet crystals. Yield: 0.435 g (74%). Anal. Calcd for $C_{18}H_{28}Cl_2NiN_6O_8$: C, 36.89; H, 4.82; N, 14.34; Cl, 12.10. Found: C, 36.76; H, 4.81; N, 14.39; Cl, 12.07.

{[Fe_2(μ-O)(μ-OAc)$_2$]$_2$(μ-bpteta)$_2$}(ClO_4)$_4$ (4). To an aqueous solution (10 mL) of bpteta·4HCl·H_2O (0.492 g, 1 mmol) and sodium acetate trihydrate (0.524 g, 4 mmol) was added $FeCl_3$·$6H_2O$ (0.540 g, 2 mmol). $NaClO_4$ (0.5 g) was added to the solution after stirring the dark brown solution for 10 min. The dark green precipitate that formed immediately was separated by decantation and dissolved in acetonitrile. Slow evaporation of the acetonitrile solution yielded dark-green hexagonal-shaped crystals. Yield: 0.120 g (16%). Anal. Calcd for $C_{44}H_{68}Cl_4Fe_4N_{12}O_{26}$: C, 34.18; H, 4.43; N, 10.87; Cl, 9.17. Found: C, 34.24; H, 4.46; N, 10.95; Cl, 9.11.

X-ray Structure Determinations. The structures of the complexes were determined at room temperature (295 K) on a Nicolet R3m/V diffractometer equipped with a molybdenum tube [$\lambda(K\alpha_1)$ = 0.709 26 Å; $\lambda(K\alpha_2)$ = 0.713 54 Å] and a graphite monochromator. Crystal data and experimental parameters are presented in Table 1. The data were corrected for Lorentz–polarization effects and absorption. The structures were solved by direct methods or Patterson techniques and refined by least-squares techniques; the programs used were from the SHELXTL system.[14]

[Fe(bpteta)](ClO_4)$_2$ (1). The complex crystallizes in the centrosymmetric monoclinic space group $P2_1/c$ with four mononuclear cations in the unit cell. All hydrogen atoms were located in a Fourier synthesis and their positions refined isotropically. All non-hydrogen atoms were refined anisotropically. The final values of the conventional R factors were R = 0.0396 and R_w = 0.0461, on the basis of 1469 independent reflections with $F > 6\sigma(F)$. The final values of the atomic positional parameters with their estimated standard deviations are listed in Table 2.

[Mn(bpteta)](ClO_4)$_2$ (2). This complex also crystallizes in the centrosymmetric monoclinic space group $P2_1/c$ with four mononuclear cations in the unit cell. All hydrogen atoms were located in a Fourier synthesis and their positions refined isotropically. All non-hydrogen atoms were refined anisotropically. The final values of the conventional R factors were R = 0.0585 and R_w = 0.0776, on the basis of 2482 independent

Table 1. Crystallographic and Data Collection Parameters for the Complexes

	1	2	3	4
formula	$C_{18}H_{28}Cl_2FeN_6O_8$	$C_{18}H_{28}Cl_2MnN_6O_8$	$C_{18}H_{28}Cl_2NiN_6O_8$	$C_{44}H_{68}Cl_4Fe_4N_{12}O_{26}$
fw	583.2	582.3	586.1	1546.3
crystal size, mm^3	0.10 × 0.20 × 0.24	0.20 × 0.24 × 0.60	0.16 × 0.20 × 0.22	0.20 × 0.40 × 0.60
T, K	295	295	295	295
space group	$P2_1/c$	$P2_1/c$	$P2_1/c$	$C2/c$
a, Å	12.496(2)	13.869(3)	12.507(3)	23.414(5)
b, Å	12.148(2)	8.710(2)	12.307(2)	22.669(5)
c, Å	16.800(3)	20.710(4)	16.777(3)	14.017(3)
β, deg	109.12(3)	91.07(2)	108.80(3)	105.77(2)
V, Å^3	2409.6(7)	2501.3(9)	2444.6(8)	7160(3)
Z	4	4	4	4
d_{calc}, Mg m^{-3}	1.608	1.546	1.592	1.434
μ, mm^{-1}	0.904	0.796	1.068	1.022
2θ, range, deg	4–45	4–50	4–45	4–53
NO[a]	3147	4441	3193	7482
NO [$F > 6\sigma(F)$]	1469	2482	1773	2839
R[b]	0.0396	0.0585	0.0341	0.0697
R_w[c]	0.0461	0.0776	0.0349	0.0954
S	1.05	1.78	1.20	1.45

[a] NO = number of observed reflections. [b] $R = \sum||F_o| - |F_c||/\sum|F_o|$. [c] $R_w = [\sum w(|F_o| - |F_c|)^2/\sum w|F_o|^2]^{1/2}$.

(12) (a) Collins, M. A.; Hodgson, D. J.; Michelsen, K.; Pedersen, E. *J. Chem. Soc., Chem. Commun.* **1987**, 1659–1660. (b) Towle, D. K.; Botsford, C. A.; Hodgson, D. J. *Inorg. Chim. Acta* **1988**, *141*, 167–168. (c) Goodson, P. A.; Hodgson, D. J. *Inorg. Chem.* **1989**, *28*, 3606–3608. (d) Oki, A. R.; Glerup, J.; Hodgson, D. J. *J. Am. Chem. Soc.* **1990**, *29*, 2435–2441. (e) Goodson, P. A.; Oki, A. R.; Glerup, J. Hodgson, D. J. *Inorg. Chem.* **1990**, *112*, 6248–6254. (f) Goodson, P. A.; Glerup, J.; Hodgson, D. J.; Michelsen, K.; Pedersen, E. *Inorg. Chem.* **1990**, *29*, 503–508. (g) Goodson, P. A.; Hodgson, D. J.; Michelsen, K.; Weihe, H. *Inorg. Chim. Acta* **1992**, *197*, 141–147. (h) Arulsamy, N.; Glerup, J.; Hodgson, D. J. *Inorg. Chem.*, in press.

(13) (a) Arulsamy, N.; Hodgson, D. J.; Glerup, J. *Inorg. Chim. Acta* **1993**, *209*, 61–69. (b) Arulsamy, N.; Goodson, P. A.; Hodgson, D. J.; Glerup, J.; Michelsen, K. *Inorg. Chim. Acta* **1994**, *216*, 21–29.

(14) Sheldrick, G. M. *SHELXTL-PLUS Crystallographic System*, Version 2; Nicolet XRD Corp.: Madison, WI, 1987.

Table 2. Atomic Coordinates (×10⁴) and Equivalent Isotropic Displacement Coefficients (Å² × 10³) for **1**

	x	y	z	U(eq)[a]
Fe(1)	2603(1)	1901(1)	910(1)	38(1)
N(1)	2539(5)	788(6)	1768(4)	42(3)
N(2)	2359(8)	543(6)	167(5)	53(4)
N(3)	4235(6)	1617(7)	1127(5)	50(4)
N(4)	3200(7)	3197(7)	1692(5)	49(3)
N(5)	2487(7)	2989(7)	−29(5)	52(4)
N(6)	995(6)	2316(6)	648(5)	45(3)
C(1)	2860(8)	894(10)	2607(6)	53(4)
C(2)	2872(10)	18(12)	3139(7)	71(6)
C(3)	2527(9)	−1002(12)	2806(8)	71(6)
C(4)	2154(8)	−1116(9)	1947(7)	56(5)
C(5)	2170(7)	−221(8)	1455(5)	43(4)
C(6)	1796(9)	−289(9)	513(6)	57(5)
C(7)	3496(11)	198(11)	130(8)	63(6)
C(8)	4384(11)	445(10)	943(8)	66(6)
C(9)	4889(9)	2020(11)	1979(6)	60(5)
C(10)	4484(10)	3127(11)	2082(8)	70(5)
C(11)	2790(11)	4209(9)	1190(7)	59(6)
C(12)	2993(11)	4061(10)	354(7)	60(5)
C(13)	1314(10)	3079(12)	−569(7)	69(5)
C(14)	567(8)	2939(8)	−44(6)	55(4)
C(15)	−516(10)	3381(9)	−253(9)	74(6)
C(16)	−1175(10)	3191(11)	235(11)	88(7)
C(17)	−745(11)	2552(10)	914(10)	77(7)
C(18)	335(9)	2161(8)	1135(8)	54(5)
Cl(1)	5471(2)	2071(2)	4483(1)	52(1)
O(1)	4409(5)	2611(6)	4204(4)	75(3)
O(2)	6168(5)	2505(7)	4059(4)	101(4)
O(3)	5969(6)	2238(8)	5348(4)	115(4)
O(4)	5299(8)	966(7)	4270(6)	141(6)
Cl(2)	1305(3)	4780(3)	2815(2)	80(1)
O(5)	584(8)	4827(9)	2004(5)	142(5)
O(6)	707(6)	4771(7)	3396(4)	107(4)
O(7)	1933(9)	3811(9)	2921(6)	153(6)
O(8)	2078(10)	5656(10)	2968(7)	182(7)

[a] Equivalent isotropic U defined as one-third of the trace of the orthogonalized U_{ij} tensor.

Table 3. Atomic Coordinates (×10⁴) and Equivalent Isotropic Displacement Coefficients (Å² t 10³) for **2**

	x	y	z	U(eq)[a]
Mn(1)	2245	2020	1202	42(1)
N(1)	702(4)	1983(6)	1502(2)	45(2)
N(2)	2227(4)	1248(7)	2267(3)	50(2)
N(3)	3357(5)	3619(7)	1729(3)	60(2)
N(4)	2051(5)	4383(8)	701(3)	60(2)
N(5)	1925(4)	1423(9)	134(3)	60(2)
N(6)	3381(4)	305(6)	896(3)	48(2)
C(1)	−33(5)	2581(8)	1141(4)	53(2)
C(2)	−987(6)	2466(9)	1327(4)	60(3)
C(3)	−1193(6)	1776(10)	1894(4)	64(3)
C(4)	−446(6)	1203(10)	2264(4)	60(3)
C(5)	478(5)	1295(8)	2058(3)	45(2)
C(6)	1309(6)	555(10)	2424(4)	59(3)
C(7)	2458(7)	2639(11)	2649(4)	64(3)
C(8)	3389(7)	3310(13)	2425(5)	74(4)
C(9)	3098(7)	5224(10)	1568(5)	73(4)
C(10)	2888(7)	5354(12)	877(6)	80(4)
C(11)	1873(8)	4192(13)	−5(5)	84(4)
C(12)	2317(8)	2745(13)	−225(5)	79(4)
C(13)	2357(6)	−37(12)	−51(4)	67(3)
C(14)	3259(5)	−392(8)	323(3)	48(2)
C(15)	3927(7)	−1422(11)	104(5)	73(4)
C(16)	4692(8)	−1821(11)	478(6)	83(4)
C(17)	4812(6)	−1157(11)	1063(6)	78(4)
C(18)	4161(5)	−87(10)	1260(4)	61(3)
Cl(1)	348(1)	7745(2)	965(1)	64(1)
O(1)	1257(4)	8171(9)	1238(3)	102(3)
O(2)	−426(5)	8293(11)	1320(5)	149(4)
O(3)	266(7)	8300(19)	371(4)	246(8)
O(4)	239(6)	6178(10)	965(7)	197(7)
Cl(2)	6048(2)	983(3)	6544(1)	85(1)
O(5)	5696(8)	241(19)	7054(6)	239(8)
O(6)	5344(6)	1343(19)	6132(5)	226(8)
O(7)	6879(8)	573(21)	6349(6)	249(9)
O(8)	6235(21)	2299(29)	6722(15)	432(22)

[a] Equivalent isotropic U defined as one-third of the trace of the orthogonalized U_{ij} tensor.

reflections with $F > 6\sigma(F)$. The final values of the atomic positional parameters with their estimated standard deviations are listed in Table 3.

[Ni(bpteta)](ClO₄)₂ (3). This complex also crystallizes in the centrosymmetric monoclinic space group $P2_1/c$ with four mononuclear cations in the unit cell. All hydrogen atoms were located in a Fourier synthesis and their positions refined isotropically. All non-hydrogen atoms were refined anisotropically. The final values of the conventional R factors were $R = 0.0341$ and $R_w = 0.0349$, on the basis of 1773 independent reflections with $F > 6\sigma(F)$. The final values of the atomic positional parameters with their estimated standard deviations are listed in Table 4.

{[Fe₂(μ-O)(μ-OAc)₂]₂(μ-bpteta)₂}(ClO₄)₄ (4). The complex crystallizes in the centrosymmetric monoclinic space group $C2/c$ with four tetranuclear cations in the unit cell. Hydrogen atoms on the secondary amino nitrogens were located in a Fourier synthesis and their positions refined isotropically. All other hydrogens were placed in calcualted positions (C–H = 0.96 Å) while non-hydrogens were refined anisotropically. The final values of the conventional R factors were $R = 0.0697$ and $R_w = 0.0954$, on the basis of 2839 independent reflections with $F > 6\sigma(F)$. The final values of the atomic positional parameters with their estimated standard deviations are listed in Table 5.

Physical Measurements. Electronic absorption spectra were recorded on a Perkin-Elmer Lambda 9 spectrophotometer in acetonitrile solvent. Magnetic susceptibility measurements were performed by the Faraday method on equipment described elsewhere.[12] The molar susceptibilities were corrected for ligand diamagnetism using Pascal's constants. Cyclic voltammograms were recorded on a BAS 100A electrochemical analyzer in acetonitrile, using a glassy-carbon working electrode, a Pt-wire auxiliary electrode, and a Ag/AgCl reference electrode. Solutions were approximately 1 mM with 0.1 M tetraethylammonium perchlorate (TEAP) as supporting electrolyte.

Results and Discussion

Syntheses. The ligand, 1,10-bis(2-pyridylmethyl)-1,4,7,10-tetraazadecane, bpteta, was synthesized as its tetrahydrochloride salt by the sodium borohydride reduction of the Schiff base obtained from the condensation of triethylenetetramine and pyridine-2-carboxaldehyde in ethanol (95%). The iron(II), manganese(II), and nickel(II) complexes of the ligand were synthesized by treating a methanolic suspension of the ligand hydrochloride salt and 4 equiv of sodium acetate and the corresponding perchlorate salt. The synthesis of the iron(II) complex required anaerobic conditions as formation of a violet-colored complex was observed in the presence of air. The tetranuclear iron(III) complex was synthesized by the reaction of an aqueous solution of the ligand hydrochloride salt with 4 equiv of sodium acetate and 2 equiv of iron(III) chloride hexahydrate. The complex was precipitated as the perchlorate salt by the addition of sodium perchlorate. Though the crude complex could be obtained almost quantitatively, recrystallization from acetonitrile resulted in considerable loss. The crystals obtained in about 16% yield were suitable for X-ray analysis and were also used for other studies.

Description of the Structures. [Fe(bpteta)](ClO₄)₂ (1) and [Ni(bpteta)](ClO₄)₂ (3). These two complexes are isomorphous, and their structures can be discussed together; each structure consists of $[M(bpteta)]^{2+}$ cations (M = Fe, Ni), which are well separated from perchlorate anions. A view of the cation in the nickel complex is given in Figure 1. Principal bond distances and anlges are listed in Tables 6 and 7 for the Fe and Ni complexes, respectively.

The $[M(bpteta)]^{2+}$ ions in these compounds have distorted octahedral coordination geometry. The ligand encapsulates the metal atom through the six ligating nitrogen atoms (two pyridyl and four secondary amine nitrogen atoms). Several isomers are possible for a ligand of this type, the one observed here having the pyridine nitrogen atoms [N(1) and N(6)] each *trans* to a secondary amine nitrogen atom [N(5) and N(3), respectively]. The bond lengths involving pyridine nitrogen atoms are not significantly different from those involving amine nitrogen atoms

Table 4. Atomic Coordinates (×10⁴) and Equivalent Isotropic Displacement Coefficients (Å² × 10³) for **3**

	x	y	z	U(eq)[a]
Ni(1)	2593(1)	1889(1)	923(1)	44(1)
N(1)	2479(4)	698(4)	1809(3)	48(2)
N(2)	2391(6)	478(4)	181(3)	60(3)
N(3)	4299(5)	1581(5)	1152(4)	58(3)
N(4)	3260(5)	3214(5)	1733(3)	59(3)
N(5)	2464(5)	3038(5)	-47(3)	59(3)
N(6)	908(4)	2338(4)	635(3)	56(2)
C(1)	2794(6)	786(7)	2652(4)	66(4)
C(2)	2825(7)	-94(9)	3157(5)	82(4)
C(3)	2528(7)	-1083(8)	2811(6)	76(4)
C(4)	2197(6)	-1185(7)	1964(6)	68(4)
C(5)	2181(5)	-289(6)	1468(4)	50(3)
C(6)	1838(8)	-343(7)	533(5)	71(4)
C(7)	3527(8)	158(7)	170(5)	76(4)
C(8)	4402(7)	422(7)	981(5)	71(4)
C(9)	4897(7)	1978(8)	1996(5)	71(4)
C(10)	4508(7)	3127(8)	2067(5)	77(4)
C(11)	2844(9)	4188(7)	1220(5)	72(4)
C(12)	2993(7)	4065(7)	369(5)	64(4)
C(13)	1286(7)	3128(8)	-560(5)	77(4)
C(14)	516(6)	2978(6)	-41(5)	64(3)
C(15)	-548(8)	3433(6)	-247(7)	87(4)
C(16)	-1214(8)	3222(8)	228(9)	104(6)
C(17)	-831(8)	2556(8)	896(8)	88(5)
C(18)	238(6)	2146(6)	1098(5)	64(4)
Cl(1)	5432(1)	2053(1)	4466(1)	55(1)
O(1)	4390(4)	2611(4)	4188(3)	83(2)
O(2)	6151(4)	2464(5)	4049(3)	101(2)
O(3)	5924(4)	2212(5)	5333(3)	119(3)
O(4)	5243(5)	959(5)	4265(4)	140(4)
Cl(2)	-1273(2)	-282(2)	2174(1)	91(1)
O(5)	-567(6)	-238(6)	2984(3)	158(4)
O(6)	-673(5)	-295(5)	1584(3)	123(3)
O(7)	-1897(7)	-1242(7)	2066(4)	185(5)
O(8)	-2047(8)	554(8)	2005(5)	211(6)

[a] Equivalent isotropic U defined as one-third of the trace of the orthogonalized U_{ij} tensor.

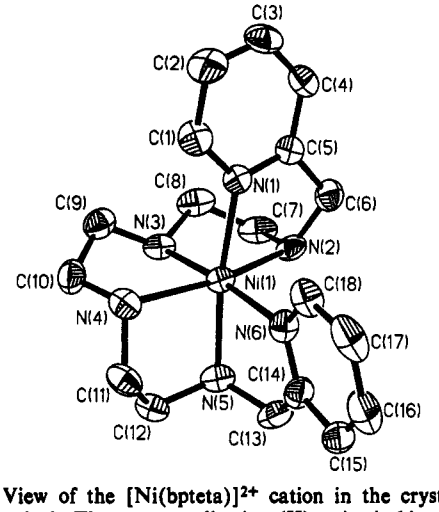

Figure 1. View of the $[Ni(bpteta)]^{2+}$ cation in the crystals of the perchlorate salt, **3**. The corresponding iron(II) cation in **1** is very similar, the crystals being isomorphous. In this and the following figures, all hydrogen atoms are omitted for clarity.

in either structure, although all metal–nitrogen bond lengths in the Ni complex are longer than those in the iron complex, reflecting the larger radius of Ni(II). The difference between the average Ni–N and Fe–N distances is 0.10(2) Å. The bond lengths found here are entirely consistent with those in other $Fe^{II}N_6$ and $Ni^{II}N_6$ chromophores.[15,16] Conversely, the five chelate bond angles of 79.8(2)–84.0(2)° [average 81.7(19)°] subtended by the ligand at the nickel atom are each smaller than their analogues of 81.5(3)–85.1(3)° [average 83.3(16)°] in the iron complex.

The perchlorate ions in both crystals are ordered and well behaved. The Cl–O bond lengths in the two crystals are in the range 1.363(5)–1.421(7) Å, with an average value of 1.396(16) Å. The O–Cl–O angles of 106.2(5)–112.8(6)° have an average value of 109.5(17)°. These values are consistent with those reported elsewhere.[17]

Table 5. Atomic Coordinates (×10⁴) and Equivalent Isotropic Displacement Coefficients (Å² × 10³) for **4**

	x	y	z	U(eq)[a]
Fe(1)	2949(1)	3351(1)	2800(1)	53(1)
N(1)	3357(5)	4125(4)	3580(8)	72(4)
N(2)	2499(6)	4113(5)	1919(7)	80(5)
N(3)	2142(4)	3408(4)	3305(6)	53(3)
N(4)	3152(4)	1598(3)	4146(6)	49(3)
N(5)	4076(5)	1353(4)	3270(7)	68(4)
N(6)	4423(3)	2196(4)	4575(6)	56(3)
O(1)	3312(3)	2846(3)	3749(4)	49(2)
O(2)	3566(4)	3383(3)	2018(6)	77(4)
O(3)	2463(3)	2795(4)	1732(5)	70(3)
Fe(2)	3618(1)	2186(1)	3387(1)	50(1)
O(4)	4083(3)	2554(3)	2479(5)	67(3)
O(5)	2976(4)	1963(3)	2150(5)	65(3)
C(1)	3702(6)	4127(6)	4496(11)	91(7)
C(2)	3967(9)	4616(8)	4963(13)	148(10)
C(3)	3897(14)	5135(10)	4356(22)	231(18)
C(4)	3535(13)	5156(8)	3461(20)	215(17)
C(5)	3300(8)	4619(6)	3071(11)	106(7)
C(6)	2938(8)	4594(6)	2019(12)	117(8)
C(7)	1994(7)	4294(7)	2310(12)	116(8)
C(8)	1725(5)	3805(6)	2642(9)	80(5)
C(9)	2258(5)	3529(5)	4369(7)	60(4)
C(10)	4541(5)	2585(5)	5318(8)	62(4)
C(11)	5064(6)	2611(7)	6026(11)	98(6)
C(12)	5511(7)	2234(8)	5958(13)	130(8)
C(13)	5417(6)	1865(7)	5167(13)	115(8)
C(14)	4859(6)	1822(5)	4479(9)	77(6)
C(15)	4723(6)	1424(6)	3633(10)	89(6)
C(16)	3859(7)	889(5)	3874(11)	91(7)
C(17)	3245(6)	985(4)	3849(10)	75(6)
C(18)	3255(5)	1703(4)	5212(7)	58(4)
C(19)	3982(5)	3029(6)	2011(8)	63(5)
C(20)	4369(6)	3188(6)	1347(10)	89(6)
C(21)	2568(5)	2261(6)	1608(7)	59(4)
C(22)	2180(6)	1958(6)	694(8)	86(6)
Cl(1)	1412(2)	1607(2)	2933(2)	75(1)
O(6)	1245(5)	1536(5)	1913(7)	125(5)
O(7)	1707(8)	2108(5)	3265(12)	199(9)
O(8)	1805(6)	1123(6)	3378(8)	157(7)
O(9)	923(5)	1540(6)	3264(9)	147(7)
Cl(2)	1441(3)	4531(2)	-715(3)	111(2)
O(10)	1999(11)	4706(11)	-351(16)	272(14)
O(11)	1104(11)	4694(10)	-46(16)	282(15)
O(12)	1335(14)	4020(10)	-806(26)	428(30)
O(13)	1310(13)	4816(17)	-1452(22)	450(26)

[a] Equivalent isotropic U defined as one-third of the trace of the orthogonalized U_{ij} tensor.

$[Mn(bpteta)](ClO_4)_2$ (2). The structure of the manganese complex consists of $[Mn(bpteta)]^{2+}$ cations and perchlorate anions. A view of the cation in the complex is given in Figure 2. Principal bond distances and angles are listed in Table 8.

The manganese ion in the complex is again coordinated to all six nitrogen atoms in the ligand, but the geometry is entirely

(15) (a) Kucharski, E. S.; McWhinnie, W. R.; White, A. H. *Aust. J. Chem.* **1978**, *31*, 53–56. (b) Oliver, J. D.; Mullica, D. F.; Hutchinson, B. B.; Milligan, W. O.; *Inorg. Chem.* **1980**, *19*, 165–169. (c) Boeyens, J. C. A.; Forbes, A. G. S.; Hancock, R. D.; Wieghardt, K. *Inorg. Chem.* **1985**, *24*, 2926–2931. (d) Christiansen, L.; Hendrickson, D. N.; Toftlund, H.; Wilson, S. R.; Xie, C.-L. *Inorg. Chem.* **1986**, *25*, 2813–2818. (e) McCusker, J. K.; Toftlund, H.; Rheingold, A. L.; Hendrickson, D. N. *J. Am. Chem. Soc.* **1993**, *115*, 1797–1804.

(16) (a) Zomba, L. J.; Margulis, T. N. *Inorg. Chim. Acta* **1980**, *45*, L264–265. (b) Thom, V. J.; Boeyens, J. C. A.; McDougall, G. J.; Hancock, R. D. *J. Am. Chem. Soc.* **1984**, *106*, 3198–3207. (c) Wieghardt, K.; Schoffmann, E.; Nuber, B.; Weiss, J. *Inorg. Chem.* **1986**, *25*, 4877–4883. (d) Bushnell, G. W.; Fortier, D. G.; McAuley, A. *Inorg. Chem.* **1988**, *27*, 2676–2684.

(17) Glerup, J.; Goodson, P. A.; Hodgson, D. J.; Lynn, M. H.; Michelsen, K. *Inorg. Chem.* **1992**, *31*, 4785–4791 and references therein.

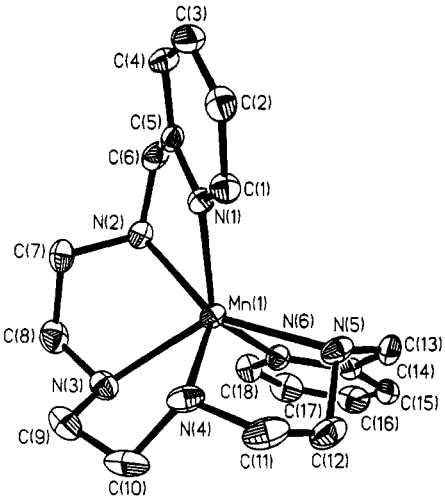

Figure 2. View of the $[Mn(bpteta)]^{2+}$ cation in the crystals of the perchlorate salt, **2**.

Table 6. Selected Bond Lengths (Å) and Bond Angles (deg) for **1**

	Bond Lengths		
Fe(1)–N(1)	1.996(8)	Fe(1)–N(2)	2.029(8)
Fe(1)–N(3)	1.981(8)	Fe(1)–N(4)	2.030(8)
Fe(1)–N(5)	2.027(9)	Fe(1)–N(6)	1.976(7)
	Bond Angles		
N(1)–Fe(1)–N(2)	82.0(3)	N(1)–Fe(1)–N(3)	91.8(3)
N(2)–Fe(1)–N(3)	84.8(4)	N(1)–Fe(1)–N(4)	98.6(3)
N(2)–Fe(1)–N(4)	167.8(4)	N(3)–Fe(1)–N(4)	83.0(3)
N(1)–Fe(1)–N(5)	173.7(3)	N(2)–Fe(1)–N(5)	95.4(3)
N(3)–Fe(1)–N(5)	93.7(4)	N(4)–Fe(1)–N(5)	85.1(3)
N(1)–Fe(1)–N(6)	93.2(3)	N(2)–Fe(1)–N(6)	97.7(3)
N(3)–Fe(1)–N(6)	174.7(3)	N(4)–Fe(1)–N(6)	94.4(3)
N(5)–Fe(1)–N(6)	81.5(3)		

Table 7. Selected Bond Lengths (Å) and Bond Angles (deg) for **3**

	Bond Lengths		
Ni(1)–N(1)	2.125(5)	Ni(1)–N(2)	2.104(6)
Ni(1)–N(3)	2.078(6)	Ni(1)–N(4)	2.115(5)
Ni(1)–N(5)	2.122(6)	Ni(1)–N(6)	2.080(5)
	Bond Angles		
N(1)–Ni(1)–N(2)	79.8(2)	N(1)–Ni(1)–N(3)	92.4(2)
N(2)–Ni(1)–N(3)	83.1(2)	N(1)–Ni(1)–N(4)	100.6(2)
N(2)–Ni(1)–N(4)	164.6(3)	N(3)–Ni(1)–N(4)	81.5(2)
N(1)–Ni(1)–N(5)	172.0(2)	N(2)–Ni(1)–N(5)	97.5(2)
N(3)–Ni(1)–N(5)	94.8(2)	N(4)–Ni(1)–N(5)	84.0(2)
N(1)–Ni(1)–N(6)	93.1(2)	N(2)–Ni(1)–N(6)	99.3(2)
N(3)–Ni(1)–N(6)	174.3(2)	N(4)–Ni(1)–N(6)	96.0(2)
N(5)–Ni(1)–N(6)	79.9(2)		

Table 8. Selected Bond Lengths (Å) and Bond Angles (deg) for **2**

	Bond Lengths		
Mn(1)–N(1)	2.240(5)	Mn(1)–N(2)	2.306(6)
Mn(1)–N(3)	2.334(6)	Mn(1)–N(4)	2.318(7)
Mn(1)–N(5)	2.307(6)	Mn(1)–N(6)	2.270(5)
	Bond Angles		
N(1)–Mn(1)–N(2)	72.7(2)	N(1)–Mn(1)–N(3)	120.3(2)
N(2)–Mn(1)–N(3)	75.2(2)	N(1)–Mn(1)–N(4)	92.0(2)
N(2)–Mn(1)–N(4)	133.2(2)	N(3)–Mn(1)–N(4)	75.5(2)
N(1)–Mn(1)–N(5)	95.5(2)	N(2)–Mn(1)–N(5)	147.8(2)
N(3)–Mn(1)–N(5)	134.2(2)	N(4)–Mn(1)–N(5)	75.6(3)
N(1)–Mn(1)–N(6)	137.7(2)	N(2)–Mn(1)–N(6)	95.4(2)
N(3)–Mn(1)–N(6)	93.9(2)	N(4)–Mn(1)–N(6)	122.3(2)
N(5)–Mn(1)–N(6)	72.9(2)		

different from that observed in the Fe(II) and Ni(II) complexes above. As is shown in Figure 3, the arrangement of the six nitrogen atoms around the metal is trigonal prismatic, the triangular faces being defined by N(1), N(4), N(5) and N(2), N(3), N(6). These

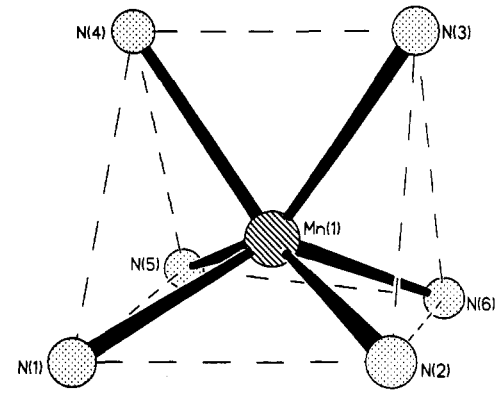

Figure 3. View of the inner sphere around the manganese center in $[Mn(bpteta)](ClO_4)_2$ (**2**) drawn to emphasize the trigonal prismatic geometry. The dotted lines indicate the outline of the trigonal prism.

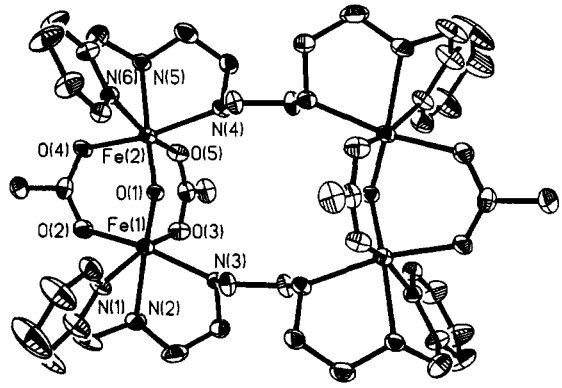

Figure 4. View of the tetranuclear $\{[Fe_2(\mu\text{-}O)(\mu\text{-}OAc)_2]_2(\mu\text{-}bpteta)_2\}^{4+}$ cation in the crystals of the perchlorate salt, **4**. Carbon atoms are unlabeled.

two triangular faces are nearly parallel, the dihedral angle between them being only 1.1°. Moreover, both triangles are nearly equilateral, the internal angles ranging from 49.6 to 66.3°.

As has been noted by Churchill and co-workers,[18] the best quantitative measure of trigonal prismatic geometry may be obtained from an examination of the relative rotational orientation of the two triangular faces. Individual twist angles ϕ in the present case are defined by N(1)–M(1)–M(2)–N(2) = 1.7°, N(4)–M(1)–M(2)–N(3) = 13.6°, and N(5)–M(1)–M(2)–N(6) = 2.1°, where M(1) and M(2) are the midpoints of the triangular faces N(1), N(4), N(5) and N(2), N(3), N(6), respectively.[18] For an idealized trigonal prism, these twist angles are 0°, while for an octahedron they would be 60°. The minor deviations from 0° observed here are primarily due to the irregularities in the Mn–N bond lenghts. Although relatively few examples exist, other workers have noted that high-spin d^5 Mn(II) complexes can accommodate this geometery more readily than ions with other electronic configurations.[19] The present structure, along with the iron and nickel structures described above, serves to underscore the enhanced tendency of manganese(II) complexes to form trigonal prismatic complexes, even in cases where the ligand can readily and demonstrably accommodate a normal pseudooctahedral arrangement.

$\{[Fe_2(\mu\text{-}O)(\mu\text{-}OAc)_2]_2(\mu\text{-}bpteta)_2\}(ClO_4)_4$ (4). The structure consists of tetranuclear $\{[Fe_2(\mu\text{-}O)(\mu\text{-}OAc)_2]_2(\mu\text{-}bpteta)_2\}^{4+}$ cations which are well separated from perchlorate anions. A view of the tetranuclear cation is given in Figure 4, and selected bond lengths and angles are compiled in Table 9.

The cation may be viewed as consisting of a dimer of dimers. The close interaction is formed between two FeN_3 units bridged

(18) Churchill, M. R.; Reis, A. H., Jr. *Inorg. Chem.* **1972**, *11*, 2299–2306.
(19) (a) Wentworth, R. A. D. *Coord. Chem. Rev.* **1972**, *9*, 171. (b) Donaldson, P. B.; Tasker, P. A.; Alcock, N. W. *J. Chem. Soc., Dalton Trans.* **1977**, 1160–1165.

Table 9. Selected Bond Lengths (Å) and Bond Angles (deg) for **4**

Bond Lengths			
Fe(1)–N(1)	2.149(9)	Fe(1)–N(2)	2.215(11)
Fe(1)–N(3)	2.192(10)	Fe(1)–O(1)	1.786(6)
Fe(1)–O(2)	2.041(10)	Fe(1)–O(3)	2.050(7)
Fe(2)–N(4)	2.175(9)	Fe(2)–N(5)	2.201(11)
Fe(2)–N(6)	2.150(7)	Fe(2)–O(1)	1.789(6)
Fe(2)–O(4)	2.063(8)	Fe(2)–O(5)	2.025(7)
Fe(1)–Fe(2)	3.067(2)		
Bond Angles			
N(1)–Fe(1)–N(2)	74.1(4)	N(1)–Fe(1)–N(3)	95.2(4)
N(2)–Fe(1)–N(3)	79.3(4)	N(1)–Fe(1)–O(1)	95.1(3)
N(2)–Fe(1)–O(1)	166.7(4)	N(3)–Fe(1)–O(1)	94.3(3)
N(1)–Fe(1)–O(2)	87.8(4)	N(2)–Fe(1)–O(2)	88.3(4)
N(3)–Fe(1)–O(2)	165.9(3)	O(1)–Fe(1)–O(2)	99.2(3)
N(1)–Fe(1)–O(3)	162.9(3)	N(2)–Fe(1)–O(3)	89.3(3)
N(3)–Fe(1)–O(3)	85.2(3)	O(1)–Fe(1)–O(3)	101.9(3)
O(2)–Fe(1)–O(3)	87.9(3)	N(4)–Fe(2)–N(5)	80.2(4)
N(4)–Fe(2)–N(6)	94.5(3)	N(5)–Fe(2)–N(6)	74.0(3)
N(4)–Fe(2)–O(1)	94.6(3)	N(5)–Fe(2)–O(1)	168.3(3)
N(6)–Fe(2)–O(1)	96.1(3)	N(4)–Fe(2)–O(4)	165.7(3)
N(5)–Fe(2)–O(4)	87.2(4)	N(6)–Fe(2)–O(4)	88.6(3)
O(1)–Fe(2)–O(4)	99.0(3)	N(4)–Fe(2)–O(5)	85.0(3)
N(5)–Fe(2)–O(5)	89.1(3)	N(6)–Fe(2)–O(5)	162.9(3)
O(1)–Fe(2)–O(5)	101.0(3)	O(4)–Fe(2)–O(5)	88.0(3)
Fe(1)–O(1)–Fe(2)	118.1(3)		

by two μ-acetato and one μ-oxo ligands, leading to a $[N_3Fe(\mu\text{-}OAc)_2(\mu\text{-}O)FeN_3]$ core reminiscent of those in several other complexes.[10,20-23] In the present case, the geometry at each iron center is roughly octahedral, with facial coordination of three nitrogen atoms from the bpteta ligands and three bridging oxygen atoms from the one μ-oxo and two μ-acetato groups. The six independent Fe–N distances are in the range 2.141(7)–2.217(10) Å, the Fe–N(pyridyl) distances of 2.141(7) and 2.148(9) Å [average 2.145(5) Å] being significantly shorter than the Fe–N(amine) bonds of 2.182(9)–2.217(10) [average 2.195(16) Å]. The bridging geometry is similar to that found in other $[Fe_2(\mu\text{-}O)(\mu\text{-}OAc)_2]$ cores. Thus, the Fe(1)–O(1) and Fe(2)–O(1) distances of 1.783(6) and 1.791(6) Å are similar to values of 1.761–1.800 Å reported for this core,[10,20-23] and the Fe–O(acetato) distances of 2.020(7)–2.050(8) Å are within the range 1.979–2.053 Å reported for other structures.[10,20-23] The Fe–O–Fe bridging angle of 118.2(4)° in the present complex is insignificantly smaller than those of 118.3–125.5° in these other complexes, but is not remarkable. The Fe···Fe separation of 3.067 Å is again similar to those of 3.064–3.168 Å in the comparable systems.

Two of these dimeric units are linked to each other by the bpteta ligands, giving rise to Fe–N–C–C–N–Fe interactions between the two iron atoms of one dimer and those of another. Consequently, the six nitrogen atoms of a given bpteta ligand bind to two different iron atoms, with one pyridine and two amine nitrogen atoms binding in a facial arrangement relative to each iron. The two binuclear units in the tetranuclear complex are identical and are related to each other by a crystallographic inversion center. Hexadentate ligands have been observed to span two metal centers in other structures, in two entirely different modes. In the binuclear manganese complex $[Mn_2O_2(O_2CCH_3)(tpen)]^{2+}$, where tpen is *N,N,N',N'*-tetrakis(2-pyridylmethyl)-1,2-ethanediamine, the two manganese centers are bridged by two μ-oxo ligands and one μ-acetato ligand, and the tpen ligand spans the two centers to provide three donors to each.[24] In the present case, however, the spanning ligand provides the only molecular pathway between the halves of the tetramer, *e.g.* between Fe(1) and Fe(2'); a similar arrangement has been observed in the related $[Fe_2(\mu\text{-}O)(\mu\text{-}OAc)_2]$ systems with 1,4-bis(1,4,7-triaza-1-cyclononyl)butane[22] and tetrakis(2-pyridylmethyl)-1,4-butanediamine (tpbn),[23] in a related glutarate-bridged system,[25] and in the manganese complex $[(Mn_2O_2)_2(tphpn)_2]^{4+}$, where tphpn is the heptadentate ligand *N,N,N',N'*-tetrakis(2-pyridylmethyl)-2-hydroxypropane-1,3-diamine.[26] The Fe···Fe separation between the cores of 7.358 Å in the present complex is shorter than those of 7.469–7.929 Å reported for the related tetranuclear iron complexes.[22,23,25] In the manganese complex, where there is a single atom bridge between the two metals, the separation of 3.971 Å is much shorter than in these iron systems, of course.[26]

Table 10. Electronic Spectral, Magnetic, and Electrochemical Data for **1–4**

complex	λ_{max}, nm (ϵ, M^{-1} cm^{-1})	μ_{eff}, μ_B	$E_{1/2}$,[a] V	ΔE, mV
1	447 (4430), 421 (sh), 585 (318)	1.385	+0.750	130
2		6.121	+1.100	200
3	522 (10), 806 (15), 878 (sh)	3.058	+1.435	140
4[b]	340 (4680), 418 (sh), 465 (810), 510 (490), 545 (sh), 730 (46)	3.200	–0.620	irrev

[a] With reference to Ag/AgCl. [b] ϵ and μ values per iron(III).

Electronic Spectra. The spectra were measured for the complexes in acetonitrile solvent in the 300–1200-nm region. The spectral data together with room-temperature magnetic moment and electrochemical data are listed in Table 10. The spectrum of the iron(II) complex, **1**, is dominated by a strong metal → ligand charge-transfer band centered at 447 nm having a shoulder at 421 nm characteristic of low-spin iron(II) complexes.[15c,16c] A band of moderate intensity is observed at 585 nm attributable to a $^1T_{1g} \leftarrow {}^1A_{1g}$ transition.[27] The spectrum of **2** did not exhibit any band in the 400–1200-nm region, commensurate with the absence of spin-allowed transitions for manganese(II). The spectrum of **3** is similar to those reported for other nickel(II) complexes.[27,28] The three weak bands observed at 522, 806, and 878 nm are assigned to the $^3T_{1g}(P) \leftarrow {}^3A_{2g}(F)$, $^3T_{1g}(F) \leftarrow {}^3A_{2g}(F)$, and $^3T_{2g}(F) \leftarrow {}^3A_{2g}(F)$ transitions.[29] The transition $^3T_{1g}(F) \leftarrow {}^3A_{2g}(F)$ represents the crystal field splitting of the ligand ($10Dq$) corresponding to the value of *ca.* 11 400 cm^{-1} for **3**. In general, the crystal field splitting energies ($10Dq$) of the ligand in nickel(II) and high-spin iron(II) complexes are comparable.[29] Absence of any absorption maximum in the 11 000–12 000-cm^{-1} region for the iron(II) complex is again commensurate with the observed magnetic moment of 0.55 μ_B (*vide infra*) for **1**. The tetranuclear iron(III) complex, **4**, exhibits rich electronic spectral features in the 400–550-nm-wavelength region similar to those of azidomethemerythrin[2a] and other model systems.[22,23,25] Another band observed for **4** at 730 nm is attributable to ligand field transitions.

Magnetic Properties. The temperature dependence of the magnetic susceptibility of a powdered sample of the tetranuclear complex **4** was measured in the range 5–291 K. As is shown in Figure 5 for complex **4**, the effective magnetic moment at room temperature is approximately 3.2 μ_B, declining monotonically to

(20) Armstrong, W. H.; Spool, A.; Papaefthymiou, G. C.; Frankel, R. B.; Lippard, S. J. *J. Am. Chem. Soc.* **1984**, *106*, 3653–3667.
(21) Hartman, J. R.; Rardin, R. L.; Chaudhuri, P.; Pohl, K.; Wieghardt, K.; Nuber, B.; Weiss, J.; Papaefthymiou, G. C.; Frankel, R. B.; Lippard, S. J. *J. Am. Chem. Soc.* **1987**, *109*, 7387–7396.
(22) Sessler, J. L.; Sibert, J. W.; Lynch, V. *Inorg. Chem.* **1990**, *29*, 4143–4146.
(23) Toftlund, H.; Murray, K. S.; Zwack, P. R.; Taylor, L. F.; Anderson, O. P. *J. Chem. Soc., Chem. Commun.* **1986**, 191–193.
(24) Pal, S.; Gohdes, J. W.; Wilisch, W. C. A.; Armstrong, W. H. *Inorg. Chem.* **1992**, *31*, 713–716.
(25) Sessler, J. L.; Sibert, J. W.; Lynch, V.; Markert, J. T.; Wooten, C. L. *Inorg. Chem.* **1993**, *32*, 621–626.
(26) Chan, M. K.; Armstrong, W. H. *J. Am. Chem. Soc.* **1991**, *113*, 5055–5057. Kirk, M. L.; Chan, M. K.; Armstrong, W. H.; Solomon, E. I. *J. Am. Chem. Soc.* **1992**, *114*, 10432–10440.
(27) (a) Wilson, L. J.; Georges, D.; Hoselton, M. A. *Inorg. Chem.* **1975**, *14*, 2698–2975. (b) Hancock, R. D.; McDougall, G. J. *J. Chem. Soc., Dalton Trans.* **1977**, 67–70.
(28) Larsen, E.; LaMar, G. N.; Wagner, B. E.; Parks, J. E.; Holm, R. H. *Inorg. Chem.* **1972**, *11*, 2652–2668.
(29) Wieghardt, K.; Schmidt, W.; Herrmann, W.; Kuppers, H.-J. *Inorg. Chem.* **1983**, *22*, 2953–2956.

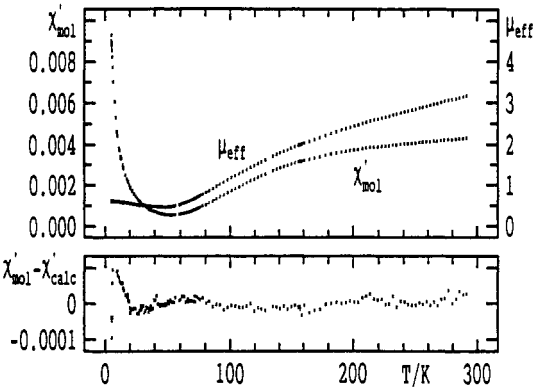

Figure 5. Magnetic susceptibility (left scale) and effective magnetic moment (right scale) for the complex $\{[Fe_2(\mu\text{-}O)(\mu\text{-}OAc)_2]_2(\mu\text{-bpteta})_2\}(ClO_4)_4$ (**4**). The lower curve shows the fit of the susceptibility data to the values calculated using the parameters $g = 2.017$, and $2J = -240.1$ cm^{-1}.

a value of 0.60 μ_B at 5 K. These properties are consistent with the existence of a singlet ground state in the complex. The room-temperature moment of 3.2 μ_B is indicative of strong antiferromagnetic interaction between the iron centers, since in a noninteracting binuclear high-spin ($S = {}^5/_2, {}^5/_2$) iron(III) system the room-temperature moment would be expected to be $\sqrt{140}$, or approximately 11.8 μ_B.

As was the case for other tetranuclear iron(III) complexes of this type, the magnetic properties for **4** were treated as being due to the presence of magnetically noninteracting binuclear units. Consequently, the temperature dependence of the magnetic susceptibility was approximated by the expression

$$\chi_{mol,exp} \simeq \chi_{mol,calc} = -\frac{N}{H}\frac{\sum_i \frac{\partial E_i}{\partial H}\exp(-E_i/kT)}{\sum_i \exp(-E_i/kT)} + K + C/T$$

by minimization of the function

$$\sum_T \frac{[\chi'_{mol,exp}(T) - \chi'_{mol,calc}(T)]^2}{\sigma^2(\chi') + \left(\frac{\partial \chi}{\partial_T}\right)^2 \sigma^2(T)}$$

within the framework of regression analysis. The term C/T accounts for the presence of small quantities of (presumably monomeric) paramagnetic impurities, while K accounts for temperature-independent paramagnetism (TIP) and for any minor deviations in the corrections for the diamagnetism of the atoms. The energies E_i of the various components of the ground-state manifold were obtained using the Hamiltonian operator

$$H = -2J(\hat{S}_1 \cdot \hat{S}_2) + g_1\beta\hat{S}_1 \cdot \hat{H} + g_2\beta\hat{S}_2 \cdot \hat{H}$$

where we have assumed that the g values for the two iron atoms are identical; *i.e.*, we have set $g_1 = g_2$. Since we have two $S = {}^5/_2$ centers in the complexes, the Heisenberg term $-2J(\hat{S}_1 \cdot \hat{S}_2)$ in the Hamiltonian gives rise to states with $S = 0, 1, 2, 3, 4$, and 5, with energies of $0, -2J, -6J, -12J, -20J$, and $-30J$, respectively. For the μ-oxo bis(μ-acetato) complex **4**, the fitting leads to a value of $2J = -240.1(3)$ cm^{-1} with $g = 2.017(2)$, $K = -5.58 \times 10^{-4}$, and impurities equivalent to 1.1% monomeric iron(III); this observed J value of -120 cm^{-1} for **4** is very similar to those of -113 and -120 recently reported for analogous tetranuclear systems[23,25] and to those of -119 and -121 for the binuclear (μ-oxo)bis(μ-acetato)diiron(III) complexes.[19,20] These J values are comparable to the value of -134 cm^{-1} reported for methemerythrin.[30]

Table 11. Structural and Magnetic Properties for Triply-Bridged Iron(III) Complexes of the Type $[Fe_2(L)_2(\mu\text{-}O)(\mu\text{-}OAC)_2]^{n+}$

L	ϕ,[a] deg	Fe–O,[b] Å	Fe···Fe, Å	$-J$, cm^{-1}	ref
bpteta[c]	118.2	1.787	3.067	120	this work
$HBpz_3$[d]	123.6	1.784	3.146	121	20
MTACN[e]	119.7	1.800	3.12	119	21
Bis(TACN)b[f]	119.8	1.777	3.076		22
tbpn[g]	121.3	1.794	3.129	120	23
TACN[h]	118.3	1.785	3.064		10
bpy[i]	123.9	1.785	3.151	132	32
tmip[j]	122.7	1.800	3.158	120	11a

[a] Fe–O–Fe bridging angle. [b] Average distance to oxo ligand. [c] 1,10-bis(2-pyridylmethyl)-1,4,7,10-tetraazadecane. [d] Hydrotris(1-pyrazolyl)-borate. [e] 1,4,7-Trimethyl-1,4,7-triazacyclononane. [f] 1,4-Bis(1,4,7-triaza-1-cyclononyl)butane. [g] *N,N,N',N'*-Tetrakis(2-pyridylmethyl)-1,4-butanediamine. [h] 1,4,7-Triazacyclononane. [i] 2,2'-Bipyridine. [j] Tris(*N*-methylimidazol-2-yl)phosphine.

Complex **4** provides another example of a (μ-oxo)bis(μ-acetato)diiron(III) complex whose Fe–O–Fe bond angle (ϕ) is smallest yet reported but whose J value is indistinguishable from those of all other analogues. Hence, the present observations support the earlier conclusion of Armstrong and co-workers[20] that there is no significant correlation between J and either ϕ or any other structural feature in complexes of this type; a similar result has been documented for other diiron(III) cores.[13,31] The magnetic and structural parameters of the triply-bridged (μ-oxo)bis(μ-acetato)diiron(III) cores in a variety of complexes are compared with those in **4** in Table 11.

The effective magnetic moment of the mononuclear iron(II) complex **1** is 0.30 μ_B at 80 K and rises gradually to 0.55 μ_B at 310 K, suggesting that the complex is a temperature-dependent mixture of predominantly low-spin (diamagnetic) and high-spin (paramagnetic) complexes. The room-temperature effective magnetic moments of **2** and **3** are 6.121 and 3.058 μ_B, respectively, indicating that the Mn(II) and Ni(II) complexes **2** and **3** are high-spin d^5 and d^8 systems, respectively.

Electrochemistry. The cyclic voltammograms of the three monomeric complexes **1–3** consist of quasi-reversible redox couples at +0.750, +1.100, and +1.435 V (vs Ag/AgCl in acetonitrile), respectively (Table 10) corresponding to the Fe(II) ↔ Fe(III), Mn(II) ↔ Mn(III), and Ni(II) ↔ Ni(III) processes. The present values are all significantly higher than those reported for an analogous series of complexes with tacn (1,4,7-triazacyclononane), the differences in $E_{1/2}$ values being approximately 0.7 V in each case.[29] This comparison suggests that the bpteta ligand stabilizes the lower M(II) oxidation state to a far greater extent than does tacn. The cyclic voltammogram of the tetranuclear complex **4** exhibits a single irreversible cathodic wave at –0.62 V, which is similar to the behavior of other known $[Fe_2(\mu\text{-}O)(\mu\text{-}OAc)_2]^{2+}$ complexes.[11a,20,21,25]

Conclusions

The new hexadentate ligand, 1,10-bis(2-pyridylmethyl)-1,4,7,10-tetraazadecane forms pseudooctahedral complexes with iron(II) and nickel(II) ions but a trigonal prismatic complex with manganese(II) ion. The iron(II) complex is a temperature-dependent mixture of low-spin and high-spin forms, while the nickel(II) and manganese(II) complexes exhibit spectral and magnetic properties typical of their electronic configuration. All

(30) Dawson, J. W.; Gray, H. B.; Hoenig, H. E.; Rossman, G. R.; Schredder, J. M.; Wang, R.-H. *Biochemistry* **1972**, *11*, 461–465.
(31) Norman, R. E.; Holz, R. C.; Ménage, S.; Que, L. *Inorg. Chem.* **1990**, *29*, 4629–4637.
(32) Vincent, J. B.; Huffman, H. C.; Christou, G.; Li, Q.; Nanny, M. A.; Hendrickson, D. N.; Fong, R. H.; Fish, R. H. *J. Am. Chem. Soc.* **1988**, *110*, 6898–6900.

these complexes exhibit quasi-reversible M(II)/M(III) redox couples at more positive potentials than those in other known MN_6 systems due to the higher crystal field splitting of the ligand. As expected, the ligand forms a tetranuclear iron(III) complex in aqueous solution. The tetranuclear complex contains two (μ-oxo)bis(μ-acetato)diiron(III/III) cores similar to three other model systems and exhibits spectral and magnetic properties similar to those observed for azidomethemerythrin, further supporting the relevance of the spontaneously assembling (μ-oxo)bis(μ-acetato)diiron(III/III)-core-containing complexes as potential models for the enzymes. However, the complex exhibits irreversible redox chemistry unlike the enzymes and similar to the other synthetic models, indicating that suitable modification of the bridging acetato units and the ligand system is still required to obtain reversible electrochemical behavior.

Acknowledgment. This work was supported by the National Science Foundation through Grant No. CHE-9007607 (to D.J.H.) and by the Scientific Affairs Division, North Atlantic Treaty Organization (NATO), through Grant No. CRG 910277 (to D.J.H. and J.G.).

Supplementary Material Available: Tables S1–S4 (hydrogen atom parameters) and S5–S8 (anisotropic thermal parameters) for the four structures (16 pages). Ordering information is given on any current masthead page.